atmosphere

MDPI

Article

Benchmarking Low-Cost Particulate Matter Sensors: Evaluating Performance Under Controlled Environmental Conditions Using Low-Cost Experimental Setups

Arianna Alvarez Cruz [1], Olivier Schalm [2], Luis Ernesto Morera Hernández [1], Alain Martínez Laguardia [3,*], Daniellys Alejo Sánchez [1], Mayra C. Morales Pérez [1], Rosa Amalia González Rivero [1] and Yasser Morera Gómez [4]

[1] Faculty of Chemistry, Central University "Marta Abreu" of Las Villas, Road to Camajuaní Km 5.5, Santa Clara 54830, Cuba; aacruz@uclv.cu (A.A.C.); lmorera@uclv.cu (L.E.M.H.); daniellysas@uclv.edu.cu (D.A.S.); mmoralesp@uclv.edu.cu (M.C.M.P.); rogrivero@uclv.cu (R.A.G.R.)
[2] Antwerp Maritime Academy, Noordkasteel Oost 6, 2030 Antwerpen, Belgium; olivier.schalm@hzs.be
[3] Faculty of Electrical Engineering, Central University "Marta Abreu" of Las Villas, Road to Camajuaní Km 5.5, Santa Clara 54830, Cuba
[4] Cienfuegos Center of Environmental Studies, Cienfuegos 59350, Cuba; yasser@ceac.cu
* Correspondence: amguardia@uclv.edu.cu

Abstract: Particulate matter (PM) is widely recognized as a major air pollutant with significant impacts on human health, highlighting the need for accurate monitoring. In developing countries, low-cost sensors are crucial for accessible PM monitoring, but their accuracy and reliability must first be assessed. This study benchmarked the Alphasense OPC-N3 and Next PM sensors through laboratory and field evaluations. Laboratory tests were performed in controlled conditions with HEPA-filtered air at low humidity and varying concentrations of water droplets from nebulized deionized water. A 27-day field study in Cienfuegos, Cuba, provided additional insights into real-world performance. The OPC-N3 showed susceptibility to perturbations and was more affected by outliers (especially PM_{10}), relative humidity, and interference from aqueous aerosols. In contrast, the Next PM sensor demonstrated superior stability, lower noise levels, and consistent performance across different environmental conditions. Despite a substantial price difference, both sensors provided valid measurements. Additionally, both sensors produced lognormal PM concentration distributions during field campaigns. This feature could aid in addressing the calibration stability challenges commonly associated with low-cost sensors through in situ calibration methods. While the PM measurements by affordable sensors are not perfect, they are sufficiently reliable for supporting air quality assessments in resource-limited settings.

Keywords: particulate matter; low-cost sensor; benchmarking; reliability; aqueous aerosols

Academic Editor: Pavel Kishcha

Received: 18 December 2024
Revised: 11 January 2025
Accepted: 30 January 2025
Published: 3 February 2025

Citation: Alvarez Cruz, A.; Schalm, O.; Morera Hernández, L.E.; Martínez Laguardia, A.; Alejo Sánchez, D.; Morales Pérez, M.C.; González Rivero, R.A.; Morera Gómez, Y. Benchmarking Low-Cost Particulate Matter Sensors: Evaluating Performance Under Controlled Environmental Conditions Using Low-Cost Experimental Setups. *Atmosphere* **2025**, *16*, 172. https://doi.org/10.3390/atmos16020172

1. Introduction

Marine aerosols and dust storms are just a few examples of natural sources that generate particulate matter (PM) in ambient air [1,2]. Additionally, anthropogenic sources such as power plants, waste incineration, industrial emissions, motor vehicles, or agricultural activities also contribute to PM levels in the air. Humans inhale these solid particles suspended in air, which can adversely affect their health [3–5]. For example, black carbon particles generated by internal combustion engines have been found in human placentae but may also accelerate the degradation of precious heritage objects [5,6]. This is why PM needs to be analysed.

PM is characterised by the size, shape, and chemical composition of individual particles, as well as the ratio between particle types [7,8]. However, practical air quality assessments often focus on total PM concentration per unit volume, neglecting the specific composition and properties of particles. This overall concentration is widely monitored by public agencies at air quality monitoring stations using gravimetric methods, which provide particulate mass concentrations for different size fractions [9–12]. These methods involve filtering particulate matter from air samples of specific size fractions and weighing the mass of the collected particles in a laboratory. Typical size fractions include fine inhalable particles with an equivalent aerodynamic diameter (AED) smaller than 2.5 μm ($PM_{2.5}$) and coarse inhalable particles with an AED of 10 μm or less (PM_{10}) [13,14]. While gravimetric methods provide accurate particle mass concentrations, they lack temporal resolution [15]. Optical particle counters address the temporal issue by continuously measuring the size of individual aerosols and mathematically converting the size into mass concentration [16]. Gravimetric and optical techniques are regulatory-approved methodologies for PM monitoring. Despite their high reliability and accuracy, these methods require significant investment in expensive infrastructure, demand highly trained personnel for operation, and are labour-intensive. These challenges hinder their widespread use in high-density monitoring networks [17,18].

Instead of using regulatory-approved techniques, low-cost alternatives are available [19]. Various low-cost sensors, priced under EUR 400, are now on the market and capable of monitoring PM concentrations, offering a more accessible solution for air quality monitoring [20–30].

One way to evaluate low-cost PM sensors is to determine their compliance with the indicative monitoring criteria outlined in the EU Directive 2008/50/EC. This Directive sets out specific requirements for measurement accuracy and reliability to ensure that data are suitable for the assessment of air quality concerning limit values, alert thresholds, and public information [19,23,24]. According to the Directive, the measurement uncertainty of PM, defined as the range within which the true value falls with 95% confidence divided by the average concentration multiplied by 100%, must not exceed 50%. While indicative monitoring emphasizes accuracy, other factors such as long-term stability, sensor durability, response time, and resistance to environmental conditions, including tropical climates and mechanical shocks, are equally important.

Several factors involved in evaluating the performance of PM sensors can be compensated through calibration methods. While indicative monitoring with low-cost sensors cannot achieve the accuracy of reference methods, their uncertainty can be minimized through proper calibration [31–34]. Data quality can be improved by accounting for various factors that affect sensor response, such as changing meteorological conditions, as particle size can depend on absorbed moisture content [35,36]. Additionally, particle composition may influence how the laser in the sensor scatters light. Compensating for sensor ageing is another key factor in improving data quality.

To assess their performance, the low-cost PM sensors must be benchmarked and compared to reference instruments. Studies [37–45] have shown that, while low-cost sensors generally do not perform as well as benchmark devices, some do exhibit better performance than others. An example of such a sensor is the OPC-N3 (Alphasense, London, UK). The accuracy of PM mass concentrations measured by the OPC-N3 has been investigated by several researchers [5,6,19,46–48] under various conditions. In 2023, Ref. [49] demonstrated that the OPC-N3 outperformed the Plantower PMS5003 (Plantower, Nanchang, China) in accurately measuring PM_{10} during regional dust events in Utah's Salt Lake Valley. Similarly, Ref. [50] conducted a comparative evaluation of the OPC-N3, SPS30, and SDS011 sensors with a reference instrument in uncontrolled indoor, outdoor, and mining environments.

This study revealed the strong accuracy and precision of these sensors when combined with local weather data and decision-tree calibration models. At the Racibórz site, the OPC-N3, housed within the Integrated Aerosol Monitoring Unit (IAMU) [51], exhibited strong temporal correlations with reference instruments, effectively estimating aerosol properties through advanced calibration methods. Furthermore, the OPC-N3 was evaluated for $PM_{2.5}$ monitoring during flights with a small unmanned aerial system (sUAS) [52]. It also identified biases where temperature measurements were overestimated and relative humidity measurements were underestimated.

Another promising sensor, Next PM (Tera Sensor, Rousset, France), appears to have comparable technical specifications at a lower acquisition cost. However, this sensor has not been systematically studied under controlled laboratory conditions and field settings. To address this gap, the objective of this benchmarking study is to evaluate the performance of the OPC-N3 and Next PM sensors through laboratory and field conditions. The focus is on assessing their raw measurements, considering only the algorithms used by the sensors to convert signals into PM concentrations, without applying additional calibration.

This study will enable communities, particularly those in resource-limited areas, to participate in monitoring air quality, promoting pollution awareness and the implementation of informed health risk reduction strategies. These solutions have the potential to democratize environmental data, thereby empowering governments and researchers to effectively address air pollution challenges. In addition, low-cost sensors offer a practical and cost-effective approach to sensor selection for the assembly of air quality devices. These solutions also facilitate the determination of PM levels in workplaces and manufacturing facilities, ensuring compliance with health and safety regulations. This study highlights the potential of low-cost PM sensors to contribute significantly to public health, environmental protection, and industrial innovation, striking a balance between affordability and performance.

2. Materials and Methods

2.1. Monitoring System

This study utilized a low-cost data logger based on an Arduino MEGA 2560 (Arduion, Monza, Italy) embedded development board. The custom-developed data logger shield featured a real-time clock, a memory card connector, and several connectors designed for the easy assembly and replacement of sensors from a predefined set. This flexibility allows the data logger to be configured according to specific experimental requirements. More information about the data logger can be found elsewhere [53].

The data logger configuration used for the laboratory experiment exemplifies how the system can be adapted to specific requirements. For this setup, the Alphasense OPC-N3 and Tera Next PM sensors (Table 1) were connected to the same data logger to synchronously measure particulate matter concentrations from the same air. Although both sensors include internal temperature and humidity measurements, an Adafruit AM2315 sensor was added to provide consistent external readings of temperature and relative humidity. Positioned between the two PM sensors, the AM2315 ensured identical environmental conditions for both, demonstrating the flexibility of the data logger to accommodate additional sensors as needed. The AM2315′s measurements were integrated into the data logger for subsequent statistical processing, ensuring reliable comparisons between the Alphasense OPC-N3 and Next PM sensors.

Table 1. Specifications of the studied low-cost PM sensors.

Characteristics	Alphasense OPC-N3	Tera Next PM
Particle range (μm)	0.35–40	0.3–10
Sampling interval (s)	1–30	1–60
Total flow rate (typical) (L/min)	5.5	2.5
Concentration detection range ($\mu g/m^3$)	0–2000	0–1000
Supply voltage (V)	4.8–5.2	5
Temperature range (°C)	−10–50	−20–70
Humidity range (%)	0–95	0–95
Operating life (h)	>15,000	>10,000
Size (L × W × H) (mm)	75 × 60 × 64	62 × 52 × 23
Weight (g)	<105	45
Price (EUR)	350	90

2.2. Clean Air Experiment

To assess the performance of low-cost PM sensors, a setup was required to create an environment with low relative humidity and minimal particulate matter to achieve zero air conditions. The OPC-N3 and Next PM sensors were positioned in the same temporal and spatial location to ensure synchronized particle measurements. These sensors were connected to a custom-developed data logger that facilitated simultaneous data collection. Specifically, they were placed inside a closed 11.1 L plastic container attached to opposite walls, with the air inlets of the sensors positioned at a distance of 10 cm, allowing for the monitoring of the same air volume under controlled conditions (see Figure 1a). The relative humidity and temperature sensor was attached perpendicularly to the lid of the box. Additionally, a Sunon Maglev (Sunonwealth, Kaohsiung, Taiwan) fan with a speed of 2400 rpm was installed to ensure the homogeneity of the air inside the box. The airflow rate of the fan was lower than the design airflow limit of the particle sensors. This ensured that the fan did not have a discernible impact on sensor performance. In addition, a layer of granular silica gel, with a diameter of 3 to 5 mm, was placed at the bottom of the box to absorb inside the closed box. Silica gel can absorb up to 40% of its weight in moisture [54]. It should be mentioned that PM may also be captured by the walls of the plastic box [32]. This suppresses the occurrence of liquid aerosols in the box and reduces the impact of relative humidity on sensor measurements [55]. To remove particulate matter from the ambient air inside the box, a loop was constructed using a second plastic container with identical dimensions. The second container contained a high-efficiency particulate air (HEPA) tubular filter (Figure 1b) through which the air was blown. The air was recirculated between the boxes through PTFE tubes using an AirPo pump. The experiments followed a fixed series of consecutive steps (see list below). Throughout the experiment, the sensor parameters were measured at a sampling interval of 5 s.

1. **Ambient air:** Measure the concentration of particulate matter in ambient air inside the closed box using both the OPC-N3 and Next PM sensors;
2. **Switch on the fan:** Activate the fan to homogenize the air;
3. **Remove PM from the container:** Switch on the pump to remove particulate matter from the air via the HEPA filter in the second box.

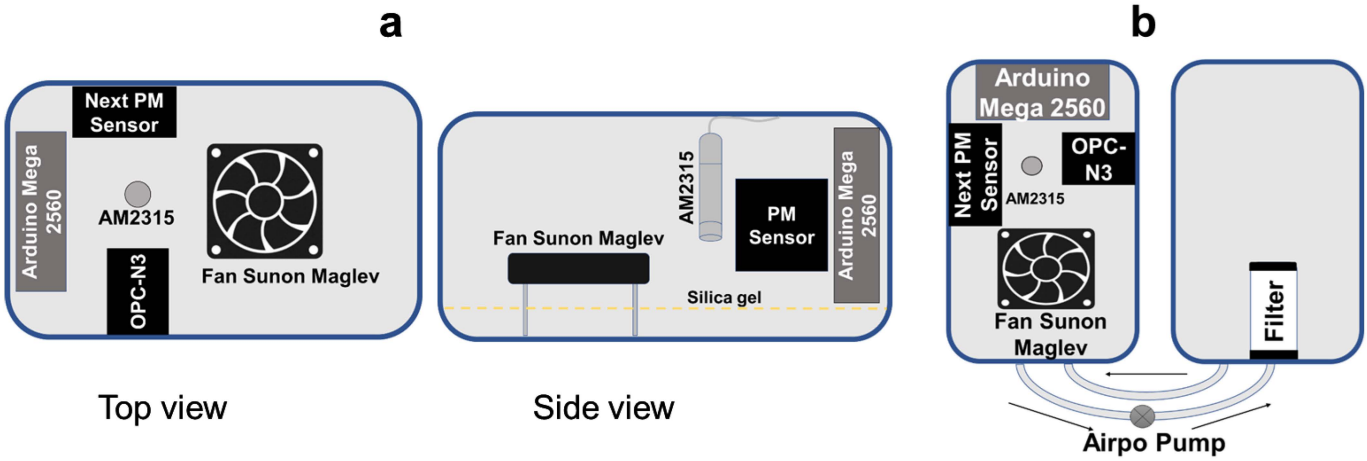

Figure 1. Schematic representation of the setup to calibrate and compare the performance of two PM sensors: (**a**) design of the box in top and side view; (**b**) design of the box and the box to remove particulate matter from the air.

2.3. Water Aerosol Experiment

To evaluate the ability of low-cost sensors to distinguish between airborne solid particles and tiny water droplets, water aerosols were introduced into a closed box using a nebulizer (Figure 2). The D2028B AirPo pump generated a pressurized airflow through 5 mL of deionized water, converting the water into tiny droplets. Consequently, 5 mL of deionized water in the form of aerosols was gradually supplied to the box. A layer of silica gel was placed at the bottom of the container to suppress an increase in relative humidity during the introduction of water aerosols. The experiments followed a series of consecutive steps (see list below), with the sensor parameters measured at a sampling time of 5 s.

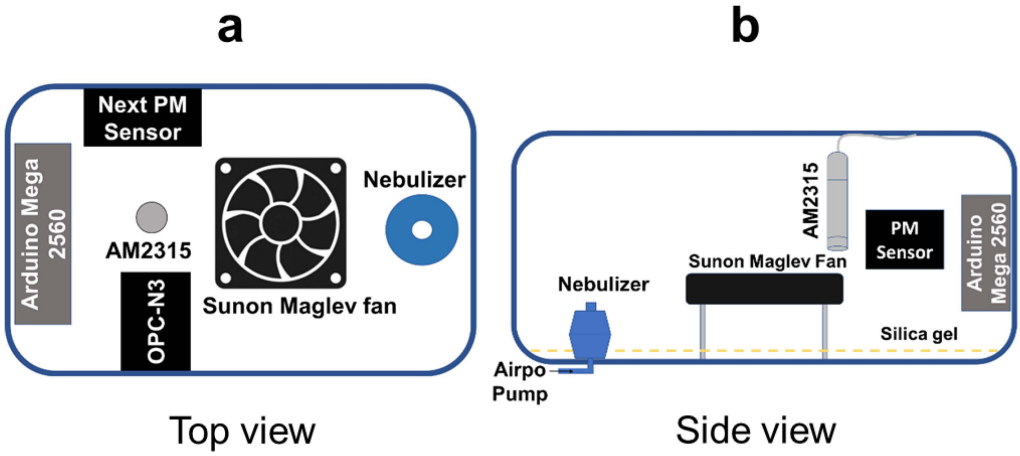

Figure 2. Schematic representation of the setup to perform water aerosol experiments: (**a**) top view and (**b**) side view.

1. **Ambient air:** The PM in the ambient air was monitored inside the open box for 10 min;
2. **Switch on fan:** After the box was closed, the fan was turned on and the environment was stabilized for 12 min;
3. **Introduce water aerosols:** The pump and the nebulizer containing deionized water were turned on for 10 min.

2.4. Field Study

A measurement campaign was carried out in Cienfuegos, on the south-central coast of Cuba, from 14 March to 9 April 2022. Cienfuegos is a city with a population of about

160,000 inhabitants. It is an important tourist centre but also an important harbour and industrial centre in Cuba [56,57]. Sampling locations for the Alphasense OPC-N3 and Next PM sensors are marked at the Center for Environmental Studies (CEAC), located 9 km south of Cienfuegos city, Cuba (22°03′55″ N, 80°28′58″ W), between the Caribbean Sea and Cienfuegos Bay (Figure 3). This site may be affected by background concentrations of PM originating from the city, emissions from the Carlos Manuel de Céspedes thermoelectric power plant, and the Camilo Cienfuegos oil refinery. Additionally, near the sampling area, there is a diesel combustion boiler and a small diesel–electric generation unit [56,58,59].

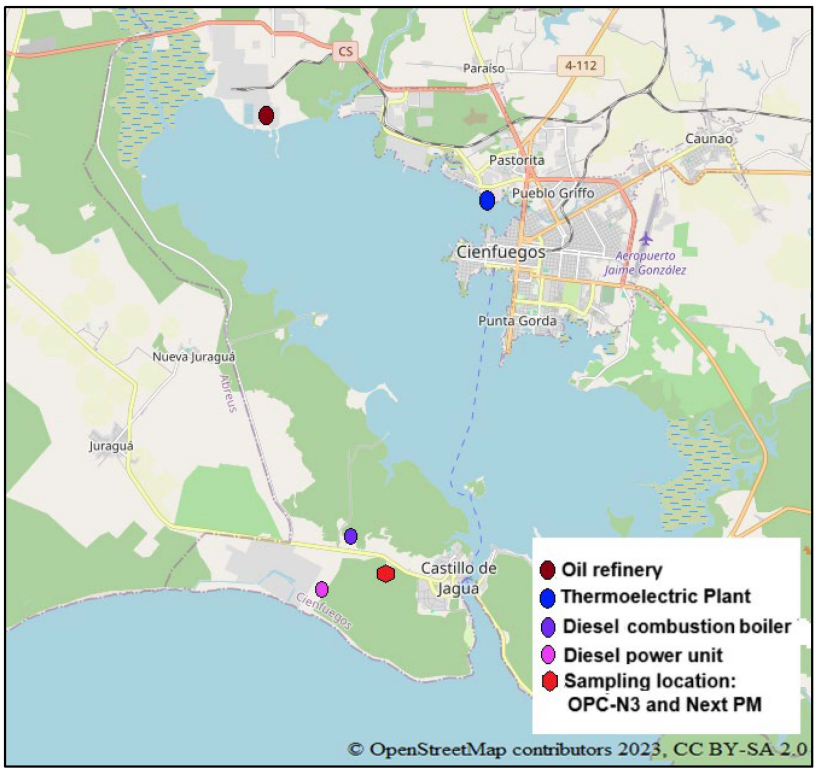

Figure 3. Location of the sampling location at CEAC and the main sources of contamination in its surroundings.

In this study, two low-cost monitoring systems were used in parallel. The first system consisted of the in-house developed HZS-GARP-AQ-03 monitoring system [60] operating at a sampling time of 5 min to which the OPC-N3 sensor was coupled. The second system consisted of the HZS-GARP-AQ-03A monitoring system to which the Next PM sensor was coupled. It operated at a sampling time of 2 min. Both systems used the Adafruit AM2315 sensor to measure temperature and relative humidity. These devices were placed outside CEAC next to a window at a height of 2 m above ground level, as prescribed by the Cuban standard NC:111 [61]. The distance between both sensors is about 0.5 m.

2.5. Data Processing

Before the field data could be analysed, erroneous outliers generated by the sensor were removed by applying a centred moving median with a window size of 10 min to the collected data. Next, the time series of both data loggers were synchronized. This was achieved by resampling the time series with the sampling interval of 2 min using the VLOOKUP function in Microsoft Excel, ensuring identical timestamps to the 5 min time series. The complex and dynamic patterns in the time series of the measured environmental parameters were revealed by time series plots. In addition, the relationship between different parameters was visualized by scatter plots. All plots were created with Microsoft Excel.

For all collected data, the average, standard deviation, asymmetry of the frequency distribution (skewness), and how much data are in the tails and the peak of the frequency distribution compared to a normal distribution (i.e., kurtosis) were calculated from the time series of the environmental parameters using the IBM SPSS Statistics 20 software package.

3. Results and Discussion

3.1. Clean Air Experiment

A primary method for the relative performance assessment of the two PM sensors is to observe their behaviour in an environment with minimal particle presence. This was achieved by drying the air presence with silica gel at the bottom of the container and removing solid particles using a HEPA filter. By creating a controlled, low-particle environment, any remaining measurements can help identify the sensors' baseline noise levels and their sensitivity to very low particulate concentrations. Temperature and relative humidity showed little variation throughout the period that the pump was switched on (step 3), with values of 25.7 ± 0.2 °C and 4.5 ± 0.1%, respectively. The behaviour of the OPC-N3 and Next PM sensors during the clean air experiment is shown in Figure 4a,b. The initial PM concentration in the box reflected the ambient air in the laboratory. When the fan was activated to homogenize the air inside the box, a sudden PM peak occurred as particles were resuspended from the bottom of the box, which was covered with silica gel granules. The peak reached values exceeding 80 μg/m^3 for $PM_{2.5}$ and 100 μg/m^3 for PM_{10} and then decreased exponentially. Although a disturbance occurred, the fan's minimal airflow remained well below the sensor's threshold, ensuring that the variations were transient and had no adverse effect on its overall performance. Once the pump was switched on and the air inside the box circulated through the HEPA filter, PM levels dropped further ($PM_{2.5}$: from 1.8 μg/m^3 to 0.36 μg/m^3; PM_{10}: from 3.4 μg/m^3 to 0.55 μg/m^3), indicating effective particle removal. The drop of about 80% suggests that the setup successfully removed a large fraction of the particles from the air inside the box. However, the setup did not produce perfect zero air, likely because the silica gel may have acted as a continuous source of particulate matter, which was progressively removed by the filter.

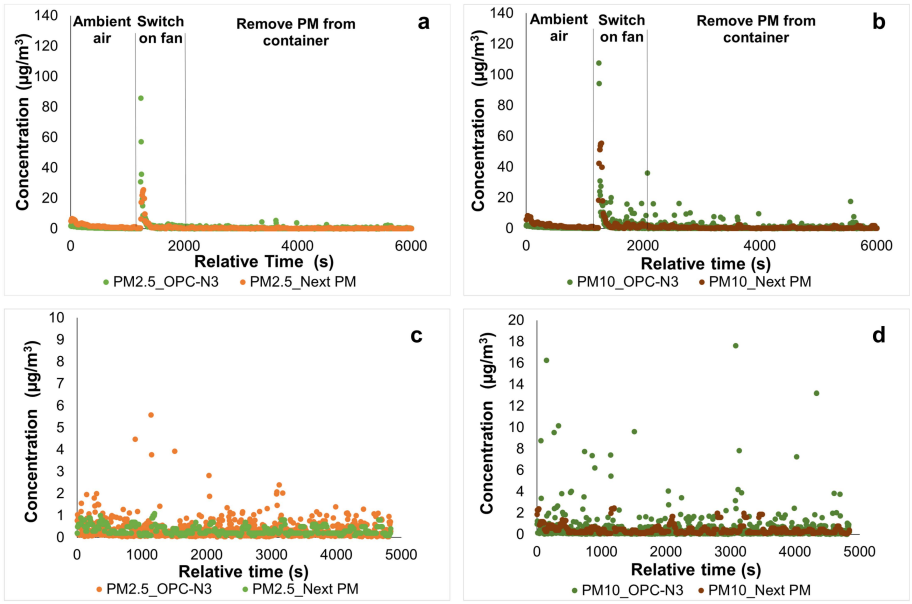

Figure 4. The results of the clean air experiments obtained by the two PM-sensors: (**a**) $PM_{2.5}$ concentrations during the entire experiment; (**b**) PM_{10} concentrations during the entire experiment; (**c**) $PM_{2.5}$ concentrations after the cleaning step with the HEPA filter; and (**d**) PM_{10} concentrations in the air after the cleaning step with the HEPA filter.

The experimental data presented in Figure 4c,d indicate that the PM concentration fluctuated around a constant average. Additionally, these fluctuations were bounded by a fixed lower limit of 0 $\mu g/m^3$, with no clearly defined upper limit. The frequency distribution of the measured concentrations is shown in Figure 5. While pollutant concentration distributions in ambient air typically follow a log-normal pattern, this distribution was not observed during the experiment. This is likely because the concentrations did not decay or increase exponentially in a random manner [62–64], but instead remained constant over time, preventing the usual variability seen in natural environments. An alternative explanation for the variation in particle concentrations around the average could be attributed to the Brownian motion of the suspended particles. If the sensors are assumed to behave as small disks that detect all particles colliding with them, and the particles move randomly within the enclosed box, then the fluctuations in the number of particles detected per unit time should follow a Poisson distribution. A similar fluctuation occurs in X-ray spectrometry, where a material emitting X-ray photons and moving towards a detector produces an X-ray spectrum governed by Poisson noise [65]. This also implies that approximately 68% of the observed values should lie within the range of $C \pm \sqrt{C}$ (average $\pm$ standard deviation). The larger spread in the measurements compared to the variation estimated from the Poisson distribution is likely attributed to outliers with unrealistically high values resulting from measurement errors. It is important to note that when the average number of hits per time unit (λ) is low, the frequency distribution is asymmetric. However, as λ increases, the distribution gradually approaches a normal distribution. This suggests that the maximum measured value during the test can serve as a performance indicator for assessing the impact of outliers on data quality generated by the PM sensors.

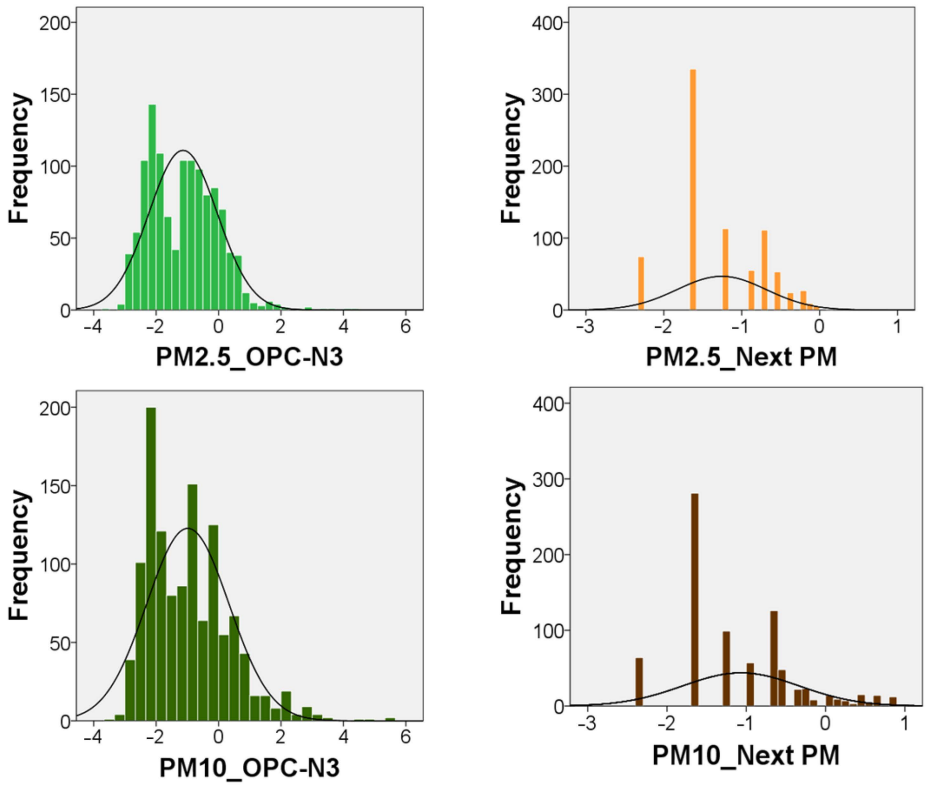

Figure 5. Frequency distribution of logarithmic values of the measured $PM_{2.5}$ and PM_{10} concentrations from step 3 of the clean air experiment. For both sensors, the distribution is shown for the raw concentrations and the logarithm of the concentrations.

A more detailed analysis of the experiment in cleaned air reveals that the average concentrations of $PM_{2.5}$ and PM_{10} are similar (see Table 2). Data distributions are not nor-

mal, which prevents the use of a t-test to determine if the means are significantly different. The OPC-N3 sensor shows a notable difference in standard deviations, particularly in its PM_{10} measurements. This increased variability is mainly due to outliers that create peaks of high concentrations, a pattern observed in other studies [66,67]. In contrast, the Next PM sensor demonstrates similar distributions for $PM_{2.5}$ and PM_{10} (see Figure 5), which differ from those recorded by the OPC-N3 sensor, as it detects a higher particle count in the same period. This difference may be related to internal mathematical filters of the Next PM sensor that processes the measured signals. In what follows, the differences are explored more in detail.

- **Concentration:** The average concentrations for $PM_{2.5}$ and PM_{10} measured by the two sensors are similar. The OPC-N3 sensor recorded an average $PM_{2.5}$ concentration of 0.4 ± 0.5 $\mu g/m^3$, which is comparable to the 0.3 ± 0.2 $\mu g/m^3$ recorded by the Next PM sensor. For PM_{10} concentrations, the OPC-N3 sensor recorded 0.6 ± 1.4 $\mu g/m^3$ while the Next PM sensor recorded 0.5 ± 0.4 $\mu g/m^3$ in the same clean air. The smaller standard deviation observed for the Next PM sensor is attributed to a lower frequency of outliers, with a maximum of 1.1 $\mu g/m^3$, compared to the OPC-N3, where $PM_{2.5}$ measurements reached up to 5 $\mu g/m^3$. This behaviour is likely due to sensor errors, which primarily impact the standard deviation. The OPC-N3 tends to produce more outliers than the Next PM sensor, and these outliers are consistently higher in value. This can be observed in the maximum concentrations measured by both sensors for $PM_{2.5}$ and PM_{10}.
- **Standard deviation:** The standard deviations of the concentration distribution are larger than anticipated, suggesting additional uncertainty. In addition, the concentration distributions illustrated in Figure 5 do not align with the assumptions of a Poisson model. The boxplot method indicates 87 outliers were recorded for the OPC-N3 and 79 for the Next PM, with maximum values of 17.6 $\mu g/m^3$ and 2.5 $\mu g/m^3$, respectively. The sensors report different particle concentration values, which are consistent despite the number of outliers detected and the large difference in maximum values. Moreover, there is no synchrony in the moments both devices detect extreme values, indicating that the elevated concentrations may be location-specific or attributable to random errors.
- **Skewness and kurtosis:** The frequency distributions of $PM_{2.5}$ and PM_{10} for both sensors show positive skewness, indicating asymmetry (see Table 2). This may be explained by a log-normal distribution. However, these distributions displayed in a semi-logarithmic graph show no clear normal distribution. Notably, the OPC-N3 sensor's distribution appears to consist of two maxima, which might indicate the occurrence of two partially overlapping particle size distributions (see Figure 5). This may result from the sensor's sensitivity to specific particle sizes, as its optical detection method amplifies certain size ranges based on size and refractive index [68]. In contrast, the Next PM sensor's measured concentrations seem to cluster around a set of discrete values. All the PM series exhibit a leptokurtic distribution (kurtosis > 3, see Table 2), indicating a higher number of outliers in the tails compared to a normal distribution. In all analyses conducted, the pronounced tails caused by these outliers lead to an asymmetric distribution. Additionally, the OPC-N3 produced a more substantial tail for PM_{10}, compared to the $PM_{2.5}$ measurements. The analyses suggest that these tails are the result of sensor errors.

Table 2. Descriptive statistics of the comparative analysis between two sensors in the experiment in cleaned air.

	AM2315	AM2315	OPC-N3	Next PM	OPC-N3	Next PM
	T [°C]	RH [%]	$PM_{2.5}$ [μg/m^3]	$PM_{2.5}$ [μg/m^3]	PM_{10} [μg/m^3]	PM_{10} [μg/m^3]
Sample size	807	807	807	807	807	807
Average	25.7	4.5	**0.4**	**0.3**	**0.6**	**0.5**
Standard deviation	0.2	0.1	0.5	0.2	1.4	0.4
Number of outliers	18	64	6	6	87	79
Minimum	25	4.2	0.0	0.10	0.0	0.10
Maximum	26	4.7	5.6	1.1	17.6	2.5
Skewness	−1.0	−1.3	4.8	1.1	6.9	2.5
Kurtosis	0.9	1.6	38.6	0.64	61.1	6.5

3.2. Water Aerosol Experiment

Another method to assess the relative performance of the two PM sensors is to observe their behaviour in an environment containing water aerosols. A nebulizer converted a small volume of water into an aerosol. Simultaneously, the bottom of the box was covered with silica gel granules to keep the RH in the box stable. Since water aerosols are not solid particles, both sensors should theoretically not respond to them. This test helps evaluate the sensors' ability to accurately differentiate between particulate matter and non-solid aerosols, providing insights into their susceptibility to false positives or measurement inaccuracies in humid conditions. Figure 6a,b show the behaviour of the sensors during the different stages of the water aerosol experiment. The PM levels varied depending on the stage of the experiment. During the ambient air step, an increase in relative humidity, $PM_{2.5}$, and PM_{10} levels was observed. After the fan was turned on, PM_{10} spikes of approximately 60 μg/m^3 were reported for the OPC-N3 sensor and 40 μg/m^3 for the Next PM sensor. When the pump was turned on and the aerosol supply to the system was initiated, a greater dispersion of the PM_{10} levels was observed. It appears that the OPC-N3 sensor considers the aerosols as particulate matter, while the Next PM sensor is less affected by the aerosols. More information is given in the list below. Therefore, exposing PM sensors to water aerosols is an effective method for assessing their performance. Water aerosols challenge the sensors' ability to differentiate between particulate matter and liquid droplets.

Table 3. Descriptive statistics of the experiment with water aerosol.

	AM2315	AM2315	OPC-N3	Next PM	OPC-N3	Next PM
	T [°C]	RH [%]	$PM_{2.5}$ [μg/m^3]	$PM_{2.5}$ [μg/m^3]	PM_{10} [μg/m^3]	PM_{10} [μg/m^3]
Sample size	431	431	431	431	431	431
Average	20.87	5.65	**1.17**	**1.73**	**5.86**	**2.18**
Standard deviation	1.15	1.15	1.48	1.66	13.51	2.13
Number of extremes	0.0	4.0	13.0	0.0	20.0	19.0
Minimum	18.9	3.6	0.0	0.0	0.0	0.0
Maximum	22.8	12.8	17.8	8.3	103.3	11.3
Skewness	0.04	2.10	6.20	1.66	3.54	1.88
Kurtosis	−1.17	13.11	58.19	2.70	14.96	3.98

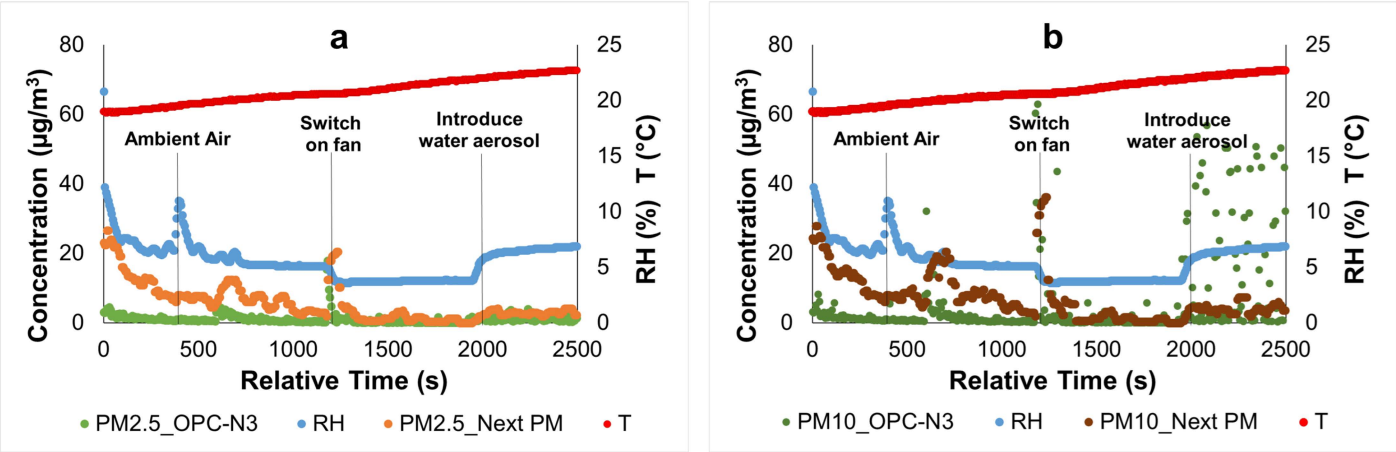

Figure 6. The behaviour of both sensors during the water aerosol experiment: (**a**) the results for the $PM_{2.5}$ measurements; (**b**) the results for the PM_{10} measurements. **Average $PM_{2.5}$ concentration:** Both sensors recorded similar $PM_{2.5}$ concentrations during the experiment, as indicated in Table 3. The mean levels during the aerosol period were 1.2 ± 1.5 µg/m^3 for the OPC-N3 sensor and 1.7 ± 1.7 µg/m^3 for the Next PM sensor. Notably, the Next PM sensor showed little difference in PM_{10} levels, suggesting that the majority of the water droplets are $PM_{2.5}$ rather than larger particles.

- **Average PM_{10} concentration**: The average PM_{10} concentration recorded by the OPC-N3 was 6 ± 14 µg/m^3 (see Table 3), which is substantially higher than the Next PM sensor, which reported lower and less dispersed values of 2.2 ± 2.1 µg/m^3. The difference between the period with the fan and the period when the nebulizer was active is quite pronounced for the OPC-N3, whereas this difference is less obvious for the Next PM sensor. This suggests that especially the OPC-N3 considers the larger droplet as particulate matter.
- **Skewness and kurtosis:** Positive skewness and positive kurtosis were observed in all the PM-related time series, indicating a more pronounced tail for larger water droplets. This suggests the presence of outliers with high concentrations or that water aerosols tend to form larger particles. However, it remains unclear whether the concentration frequency distribution follows a true lognormal distribution (see Figure 7). Further analysis is necessary to confirm the underlying distribution of the data.

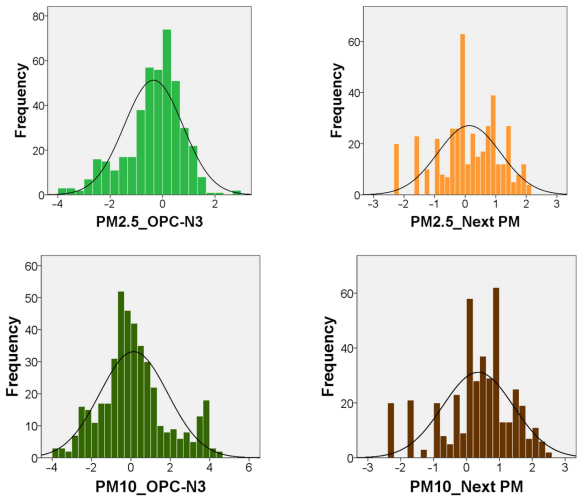

Figure 7. Log-normal PM_{10} and $PM_{2.5}$ distributions by the Next PM sensor in the water aerosol experiment. The OPC distributions demonstrate higher and broader profiles, suggesting that the OPC detects a greater number of water aerosols than the Next PM.

3.3. Field Study

Figure 8a,b show the behaviour of the meteorological variables and the concentration of particulate matter as collected by two monitoring systems measuring the same outdoor air at a short distance from each other during the field campaign in Cienfuegos. Both systems exhibited fluctuations in the studied parameters, reflecting the day and night cycles and the cycles of transport and economic activity throughout the day at the measurement location. Although a visual comparison of the PM measurements by both sensors using Figure 8c,d is not straightforward, it seems that some PM peaks measured by both sensors are in synchrony while others are not.

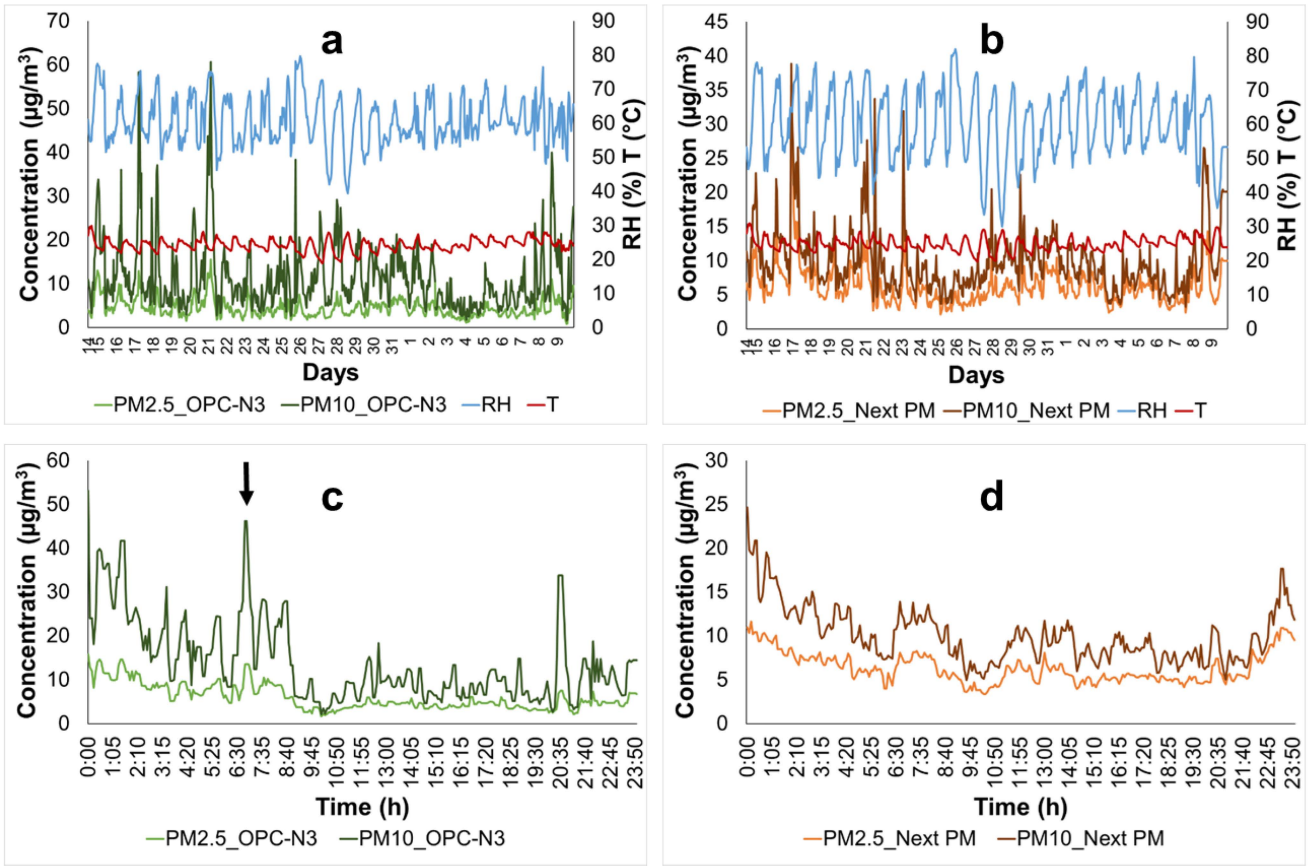

Figure 8. Monitoring results in Cienfuegos performed between March 14 and April 9, covering 27 days: (**a**) concentrations of PM_{10}, $PM_{2.5}$, RH, and T from the system containing the OPC-N3 sensor; (**b**) concentrations of PM_{10}, $PM_{2.5}$, RH, and T from the system containing the Next PM sensor; (**c**) and (**d**) details of the monitoring campaign for $PM_{2.5}$ and PM_{10} measured by the Next PM and the OPC-N3 during 24 h on 15 March.

If one assumes that peaks and valleys in the PM time series from both sensors should occur in synchrony, a high correlation between the measurements would be expected. However, as shown in Figure 9, the correlation between the two sensors is weak. For instance, the OPC-N3 detects a significant PM_{10} peak (see arrow in Figure 8c) that the Next PM sensor does not register, highlighting discrepancies in their responses to changes in particulate matter concentrations. This differing behaviour may not necessarily indicate a limitation in sensor performance but could be explained by natural phenomena. Airflow can be visualized as a horizontal stream of rotating eddies, or turbulent vortices of varying sizes, each with horizontal and vertical components. Such turbulence can lead to localized variations in PM concentration, causing differences in sensor readings. Additionally, Brownian motion may further contribute to discrepancies between the sensor measurements. These phenomena sug-

gest that the lack of synchrony between sensor outputs is not necessarily a reliable indicator to compare the performance of PM sensors. However, field evaluations using low-cost sensors such as the Purple Air PA-II have shown that sensor outputs can correlate strongly with reference measurements despite timing discrepancies. Studies [69,70] report high coefficients of determination (R^2 values ranging from 0.87 to 0.98) for $PM_{2.5}$ measurements compared with reference instruments. In this case, the higher R^2 values for $PM_{2.5}$ may be due to the OPC-N3 producing fewer outliers for these measurements than for PM_{10}.

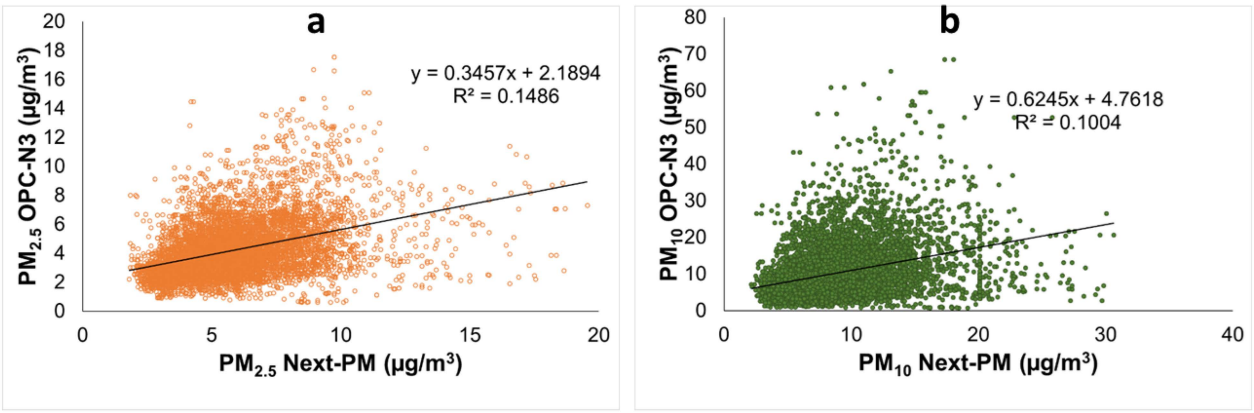

Figure 9. Relationships between the PM concentrations as measured by the OPC-N3 and the Next PM sensors: (**a**) relationship of the $PM_{2.5}$ particles between both sensors; (**b**) relationship of the PM_{10} particles between both sensors.

The statistical properties of the PM measuring campaigns as performed with both sensors are summarized in Table 4. The average $PM_{2.5}$ concentrations for the OPC-N3 and the Next PM sensors are 4 ± 3 µg/m^3 and 6 ± 4 µg/m^3, respectively. Notably, the ratio of standard deviation to mean (coefficient of variation) is identical for both sensors at 0.55, indicating similar measurement variability relative to the mean. While a constant background PM concentration may exist at a measuring location at all moments, it seems more reasonable to assume that PM concentrations fluctuate, with peaks at certain moments and concentrations close to zero at other (brief) intervals. However, for the Next PM sensor, the minimum concentration is 1.4 µg/m^3, not zero. Additionally, the maximum $PM_{2.5}$ measured by the Next PM sensor is approximately three times higher than that recorded by the OPC-N3, highlighting a notable difference in performance between the two sensors.

Table 4. Descriptive statistics of the field sample in Cienfuegos.

Parameter	HZS-GARP-AQ-03				HZS-GARP-AQ-03A			
	AM2315		OPC-N3		AM2315		Next PM	
	T	RH	$PM_{2.5}$	PM_{10}	T	RH	$PM_{2.5}$	PM_{10}
	(°C)	(%)	(µg/m^3)	(µg/m^3)	(°C)	(%)	(µg/m^3)	(µg/m^3)
Sample size	7617	7617	7617	7617	7617	7617	7617	7617
Average	24.3	60.7	**4.5**	**12.3**	24.9	60.1	**6.4**	**10.1**
Standard deviation	1.9	7.6	2.5	12.1	2.0	10.5	3.7	5.6
Number of extremes	96	10	353	418	67	2	291	348
Minimum	18.71	13.0	0.0	0.0	19.6	28.8	1.4	1.5
Maximum	30.17	84.5	21.5	394.7	31.1	83.0	68.0	77.0
Skewness	−1.180	0.1	1.7	6.7	0.3	−0.2	4.7	2.5
Kurtosis	18.439	0.1	4.4	144.2	0.1	2.5	44.1	14.0

For PM_{10}, the average concentrations for the OPC-N3 and Next PM sensors are 12 ± 12 µg/m^3 and 10 ± 6 µg/m^3, respectively. Since the concentration range of the Next PM entirely falls within the range of the OPC-N3, no distinct difference in average concentration can be noticed. However, the coefficient of variation for the OPC-N3 is greater at 0.98 compared to 0.55 for the Next PM, indicating that the OPC-N3 has greater variability in its measurements relative to its mean. The minimum measured concentration for the Next PM is not zero concentration, while the maximum concentration for the OPC-N3 is about a factor of 5 higher than for the Next PM. This is consistent with the larger variation in and occurrence of outliers observed for the OPC-N3 during the clean air experiment and the water aerosol experiment, suggesting that PM_{10} measurements performed by the OPC-N3 show greater variability.

Figure 10 displays the frequency distribution of the logarithm of the measured concentrations. The Q-Q plots suggest that the distributions closely follow a log-normal pattern with a coefficient of determination close to 1. The analysed time series exhibit positive skewness, consistent with a log-normal distribution. All PM distributions are leptokurtic, indicating that the values are concentrated around the mean but with a higher probability of extreme values. The PM_{10} measurements from the OPC-N3 exhibit a more pronounced tail, indicating a higher occurrence of elevated values. In contrast, the Next PM sensor displays a slightly more centralized distribution with reduced dispersion toward the extremes. This distinction may account for the Next PM recording slightly fewer extreme values compared to the OPC-N3. The log-normal distribution, often observed in many natural systems, arises from exponential kinetics with both deterministic and stochastic components [32,54–56]. It should be noted that the log-normal-like distribution observed in the clean air experiment and the water aerosol experiment is not due to an exponential decay or increase in local concentration, as the PM concentration remained constant over time. These distributions are merely caused by Poisson noise and random measuring errors.

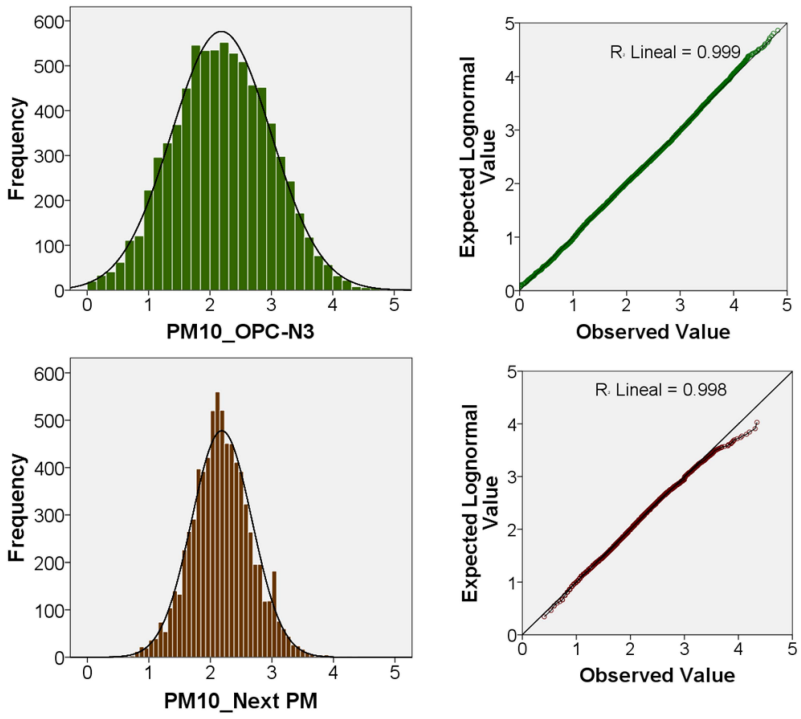

Figure 10. Frequency distribution of the measured PM_{10} concentrations from the field campaign and Q-Q plot. For both sensors, the distribution is shown for the logarithm of the concentrations. The average values are fairly similar, but the standard deviation for the OPC distribution is significantly larger.

State-of-the-art optical particle counters for environmental regulatory monitoring typically precondition the inlet air using a heated inlet. This prevents the detection of water aerosols and avoids changes in particle size when hygroscopic particles absorb or release moisture [71,72]. As a result, low-cost PM sensors are expected to observe a higher PM concentration during wet periods—because water aerosols are not distinguished from particulate matter—and larger particle sizes at higher relative humidity. The weak positive relationships in Figure 11a,b suggest that larger particles tend to be observed more frequently at higher relative humidity (RH). In addition, the OPC-N3 appears to be more affected by this phenomenon than the Next PM. This might be explained by the presence of a resistor heater inside the Next PM sensor. However, this relationship may also be partly caused by genuine relations occurring in nature. When analysing the $PM_{2.5}$:PM_{10} ratio, no decrease was observed at higher RH for either sensor. Figure 11 only shows that behaviour for the Next PM (see Figure 11c). This observation suggests that all particles grow at elevated RH so that both more $PM_{2.5}$ and more PM_{10} are present in the air. It is worth noting that the relatively weak relationship between PM concentrations and relative humidity (RH) is overshadowed by the stronger correlation between PM measurements at time *t* and the preceding measurements at time *t*-1 (see Figure 11d). The autocorrelation is caused by a rather high sampling rate at which the time series were collected that appeared to be faster than the natural changes caused by underlying mechanisms being observed, resulting in consecutive measurements showing large similarities.

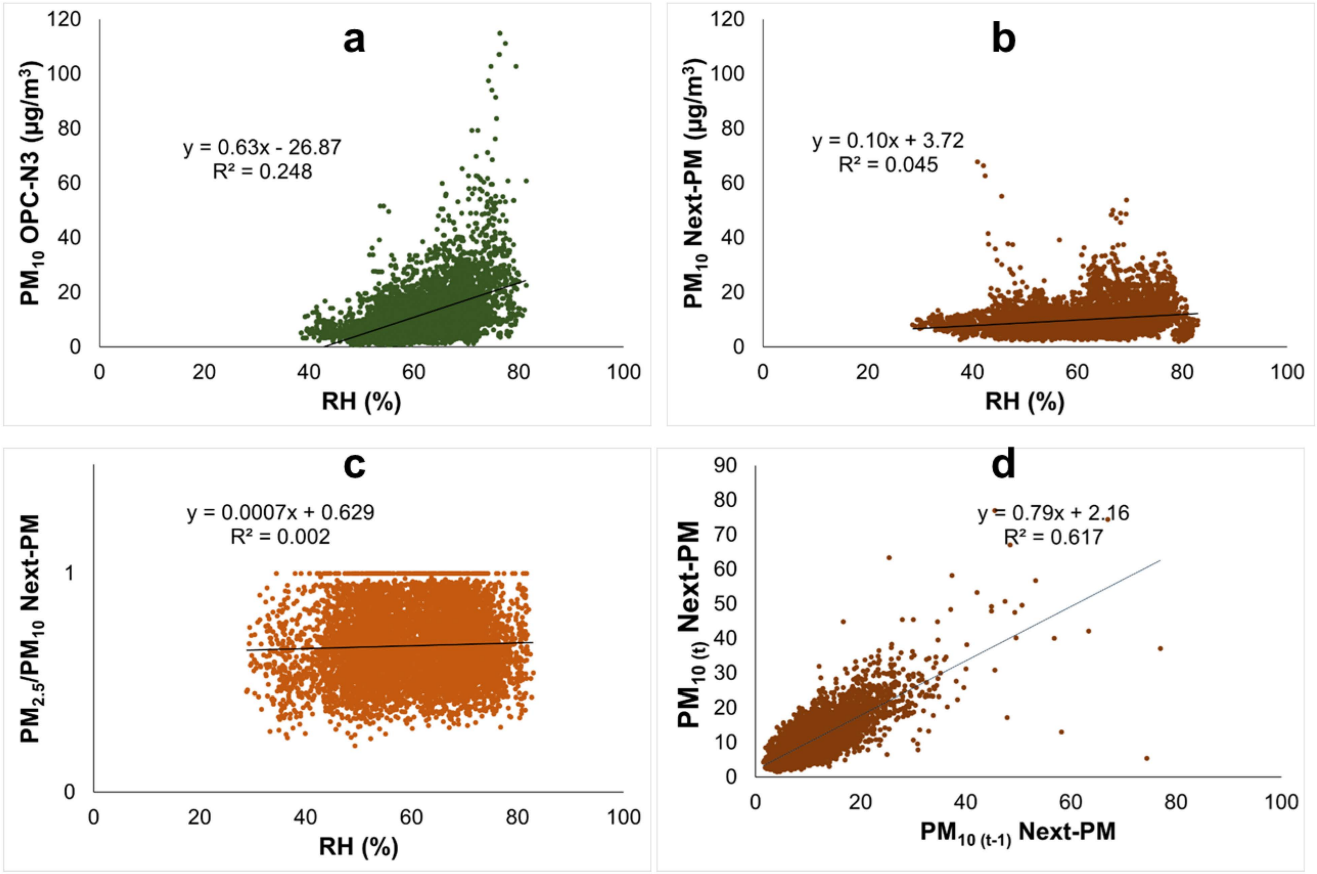

Figure 11. The relationships between PM concentration and RH: (**a**) the relationship between PM_{10} concentration and RH for the OPC-N3 sensor; (**b**) a similar relationship as in the figure as determined by the Next PM; (**c**) $PM_{2.5}$:PM_{10} ratio over RH as determined by the Next PM; and (**d**) the relationship between the PM measurement at time *t* and the preceding measurement at time *t*–1.

4. Discussion

The performance conducted through laboratory experiments and field campaigns with two different types of PM sensors identified several factors that influence the relationship between sensor measurements and the actual concentration of the target analyte. These findings are summarized in the roadmap shown in Figure 12. The impact of these factors on sensor readings plays a crucial role in determining the sensors' overall performance. These factors can also be used to compare the performance of both sensors.

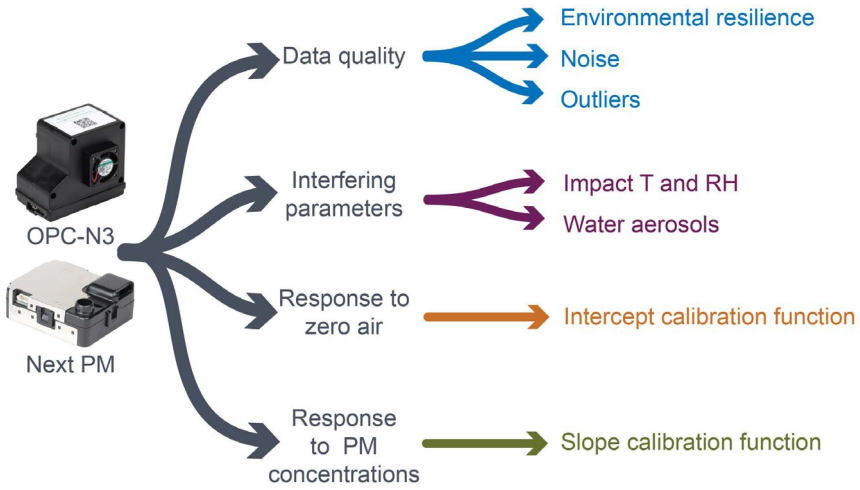

Figure 12. Overview of the roadmap containing all identified factors that affect the sensor performance.

The factors outlined in the performance assessment roadmap in Figure 12 were used to evaluate the performance of two low-cost PM sensors. Detailed results for each factor are provided below, with an overall evaluation summarized in Table 5. Table 5 compares the performance of $PM_{2.5}$ and PM_{10} measurements for both sensors separately. Although Table 5 does not include a direct comparison between the performance of $PM_{2.5}$ and PM_{10} for a single sensor, it is worth noting that PM_{10} measurements by the OPC-N3 contain substantially more outliers than the corresponding $PM_{2.5}$ measurements.

- **Environmental resilience:** Both sensors were deployed in monitoring campaigns in a tropical climate for 27 days. The harsh conditions, including high temperature, high relative humidity, and elevated salt concentrations, did not appear to have a significant effect on the sensors' performance over this short period.
- **Noise:** During the clean-air laboratory experiments, $PM_{2.5}$ and PM_{10} levels were reduced by 80% compared to ambient air concentration. The OPC-N3 sensor exhibited more fluctuations in measurements compared to the Next PM sensor (see standard deviations in Table 2). In addition, the random variation in PM_{10} measurements was larger than for $PM_{2.5}$ for both sensors.
- **Outliers:** During the clean-air laboratory experiment, the OPC-N3 sensor exhibited significantly more instances of exceptionally high values for both $PM_{2.5}$ and PM_{10}. This effect was particularly pronounced for PM_{10}. In the field study, outliers were identified as deviations from the expected lognormal distribution, especially for the larger particles in the particle size distribution. In this case, the OPC-N3 showed the highest values of standard deviation and skewness in the PM_{10} measurements. This suggests that the OPC-N3 may be more sensitive to extreme fluctuations, especially in environments with higher concentrations of larger particles.
- **Relative humidity:** Field experiments demonstrated that relative humidity had a greater impact on the OPC-N3 sensor's measurements compared to the Next PM sensor, as evidenced by a higher slope. This is likely because hygroscopic particles

change size when absorbing or releasing moisture. The steeper slope for PM_{10} indicates that variations in PM_{10} readings are more significant relative to $PM_{2.5}$. The presence of a resistance heater inside the Next PM sensor likely explains the difference in behaviour between the two sensors.

- **Impact water aerosols:** The OPC-N3 sensor demonstrated heightened sensitivity to detecting PM_{10} particles in the presence of water aerosols, indicating the potential for false positives in such conditions.
- **Response to zero air:** In clean-air laboratory experiments, both sensors registered low PM concentrations. However, the OPC-N3 tended to measure slightly higher average concentrations than the Next PM.
- **Response to PM concentrations:** Statistical analysis revealed that, although the Next PM sensor recorded lower concentrations than the OPC-N3 during the field campaign, both sensors were capable of detecting variations in pollutant levels. Both sensors recorded concentration ranges with lower limits comparable to the lowest PM concentrations observed in the clean air experiment.

Table 5. Assessment of the OPC-N3 and Next PM sensors using the identified factors for $PM_{2.5}$ and PM_{10} separately. The symbol "+" means a better performance compared to the other sensor or a better performance of one parameter ($PM_{2.5}$ or PM_{10}) relative to the other; "±" indicates a similar performance; and "-"means a worse performance. The scores associated with +, ±, and – are +1, 0, and −1, respectively.

Factor	$PM_{2.5}$		PM_{10}		Remarks
	OPC-N3	Next PM	OPC-N3	Next PM	
Environmental resilience	±	±	±	±	Similar behaviour
Noise	−	+	−	+	Next PM excels for PM_{10}
Outliers	−	+	−	+	Many outliers for PM_{10} by OPC-N3
Relative humidity	−	+	−	+	Next PM is less affected by RH
Water aerosols	−	+	−	+	OPC-N3 is more affected by aerosols
Response to zero air	±	±	±	±	No clear difference between sensors
Response to PM concentration	±	±	±	±	No clear difference between sensors
Total score	**−4**	**+4**	**−4**	**+4**	

The observed differences in performance between the OPC-N3 and Next PM sensors (Table 5) should be attributed to several key factors inherent to their design and operational characteristics. Firstly, the OPC-N3 features a more complex measurement system with 24 histogram channels, allowing for higher resolution in particle size distribution, which may lead to greater sensitivity to variations in particulate matter concentrations as demonstrated in studies by [34,49,73]. Conversely, the Next PM, while robust and equipped with a self-cleaning mechanism, operates within a narrower particle size range (0.3 µm–10 µm) and employs algorithms for environmental compensation, particularly for humidity, which may enhance its stability in adverse conditions but potentially limit its responsiveness to rapid changes in PM levels. Additionally, the components of the sensors and their respective detection techniques—laser scattering for the OPC-N3 and optical methods for the Next PM—contribute to observed discrepancies in measurement accuracy and demonstrate that the OPC-N3 is more susceptible to the disturbances that were evaluated. The results align with previous studies [51,67,74], that evaluated the OPC-N3′s performance in humid environments. These researchers reported that high relative humidity can lead to increased measurement noise and the occurrence of outliers, which can compromise the accuracy and reliability of its readings.

A key strength of this study is the rigorous control of experimental conditions, ensuring that both sensors were tested under identical conditions. This consistency ensured that

performance discrepancies were solely due to sensor-specific characteristics. The application of a unified protocol further validated the findings, with statistical analysis confirming that differences in outlier frequency and sensitivity to relative humidity stemmed from the sensors' design. These results underscore the strengths and limitations of the OPC-N3 and Next PM, reinforcing the robustness of the benchmarking framework used.

While this study does not focus on calibration, as it primarily analyses uncalibrated data using the inherent algorithms of each sensor, it is important to recognize that calibration significantly influences data quality. It enhances measurement precision and accuracy by compensating for environmental influences, addressing long-term stability challenges, and enabling effective benchmarking against reference standards. The findings of this study indicate that log-normal distributions of particle concentrations can serve as a foundation for developing both in situ and zero-point calibration algorithms. While the algorithms employed by both sensors provide a basis for interpreting raw data, establishing calibration protocols in future work is essential.

5. Conclusions

This study benchmarks the performance of two low-cost PM sensors, OPC-N3 and Next PM, under controlled laboratory conditions and during field measurements. A comprehensive set of factors affecting sensor performance was analysed, providing a robust framework for future benchmarking studies.

The findings indicate that the Next PM sensor provides measurements that are more consistent and reliable than the OPC-N3, particularly for PM_{10} data, which exhibited susceptibility to perturbations and more frequent outliers. Additionally, the Next PM sensor showed better resilience to environmental conditions, such as high relative humidity and the presence of water aerosols, reducing the likelihood of false positives. In contrast, the OPC-N3 was more susceptible to noise and variations in environmental conditions.

This study underscores the viability of conducting substantial sensor benchmarking with cost-effective configurations, thereby expanding the accessibility of air quality research. This approach fosters inclusivity in scientific initiatives, enabling resource-constrained regions to contribute to global air quality monitoring initiatives.

Future research should explore extended deployment durations and incorporate in situ calibration techniques to further refine sensor accuracy. Leveraging statistical distribution patterns of sensor outputs offers promising pathways for automated calibration and long-term reliability enhancement.

Author Contributions: A.A.C.: data processing, methodology, analysis of the results, and manuscript preparation. O.S.: conception and design of the experiments, research conception and preparation, review, editing, and approval of the final version of the manuscript. L.E.M.H.: conduct of the experimental work. A.M.L.: design of the low-cost monitoring system, review, editing, and approval of the final version of the manuscript. D.A.S.: research conception and preparation, review, and approval of the final version of the manuscript. M.C.M.P.: data processing and analysis of the results obtained. R.A.G.R.: conduct of the experimental work and review. Y.M.G.: sampling site selection strategy. All authors have read and agreed to the published version of the manuscript.

Funding: 4000 from Global Minds project, 2022GMHVLHC106, a collaborative initiative involving all Flemish Universities of Applied Sciences and Arts, 500 from Cuban Office of Management of Funds and International Projects under code PN223LH004-031.

Institutional Review Board Statement: Not applicable.

Informed Consent Statement: Not applicable.

Data Availability Statement: All data used in this study are available upon request.

Acknowledgments: The authors express their gratitude for the financial support received from the Global Minds project, 2022GMHVLHC106, a collaborative initiative involving all Flemish Universities of Applied Sciences and Arts. The research that led to the results presented in this publication received funding from the Cuban Office of Management of Funds and International Projects under code PN223LH004-031.

Conflicts of Interest: The authors declare no conflict of interest.

References

1. Xue, J.; Li, Y.; Peppers, J.; Wan, C.; Kado, N.Y.; Green, P.G.; Young, T.M.; Kleeman, M.J. Ultrafine Particle Emissions from Natural Gas, Biogas, and Biomethane Combustion. *Environ. Sci. Technol.* **2018**, *52*, 13619–13628. [CrossRef] [PubMed]
2. Dharaiya, V.R.; Malyan, V.; Kumar, V.; Sahu, M.; Venkatraman, C.; Biswas, P.; Yadav, K.; Haswani, D.; Sunder Raman, R.; Bhat, R.; et al. Evaluating the Performance of Low-Cost PM Sensors over Multiple COALESCE Network Sites. *Aerosol. Air Qual. Res.* **2023**, *23*, 220390. [CrossRef]
3. Horender, S.; Tancev, G.; Auderset, K.; Vasilatou, K. Traceable PM 2.5 and PM 10 Calibration of Low-Cost Sensors with Ambient-like Aerosols Generated in the Laboratory. *Appl. Sci.* **2021**, *11*, 9014. [CrossRef]
4. Wu, T.Y.; Horender, S.; Tancev, G.; Vasilatou, K. Evaluation of Aerosol-Spectrometer Based PM2.5 and PM10 Mass Concentration Measurement Using Ambient-like Model Aerosols in the Laboratory. *Meas. J. Int. Meas. Confed.* **2022**, *201*. [CrossRef]
5. Marchetti, A.; Pilehvar, S.; 't Hart, L.; Leyva Pernia, D.; Voet, O.; Anaf, W.; Nuyts, G.; Otten, E.; Demeyer, S.; Schalm, O.; et al. Indoor Environmental Quality Index for Conservation Environments: The Importance of Including Particulate Matter. *Build. Environ.* **2017**, *126*, 132–146. [CrossRef]
6. Bové, H.; Bongaerts, E.; Slenders, E.; Bijnens, E.M.; Saenen, N.D.; Gyselaers, W.; Van Eyken, P.; Plusquin, M.; Roeffaers, M.B.J.; Ameloot, M.; et al. Ambient Black Carbon Particles Reach the Fetal Side of Human Placenta. *Nat. Commun.* **2019**, *10*, 1–7. [CrossRef]
7. Jambers, W.; De Bock, L.; Van Grieken, R. Recent Advances in the Analysis of Individual Environmental Particles. A Review. *Analyst* **1995**, *120*, 681–692. [CrossRef]
8. Shao, L.; Liu, P.; Jones, T.; Yang, S.; Wang, W.; Zhang, D.; Li, Y.; Yang, C.X.; Xing, J.; Hou, C.; et al. A Review of Atmospheric Individual Particle Analyses: Methodologies and Applications in Environmental Research. *Gondwana Res.* **2022**, *110*, 347–369. [CrossRef]
9. Air Quality Guidelines for Particulate Matter, Ozone, Nitrogen Dioxide and Sulfur Dioxide. Available online: https://www.who.int/publications/i/item/WHO-SDE-PHE-OEH-06-02 (accessed on 11 September 2024).
10. Organización Mundial de la Salud (OMS). *WHO Global Air Quality Guidelines. Part. Matter (PM2.5 PM10), Ozone, Nitrogen Dioxide, Sulfur Dioxide Carbon Monoxide*; Organización Mundial de la Salud (OMS): Geneva, Switzerland, 2021; pp. 1–360.
11. *ISO 23210:2009*; Stationary Source Emissions—Determination of PM10/PM2. 5 Mass Concentration in Flue Gas—Measurement at Low Concentrations by Use of Impactors. International Organization for Standardization: Geneva, Switzerland, 2009. Available online: https://www.iso.org/standard/53379.html (accessed on 11 September 2024).
12. *BS EN 13284-1:2017*; Stationary Source Emissions. Determination of Low Range Mass Concentration of Dust Manual Gravimetric Method. European Commission: Brussels, Belgium, 2017. Available online: https://www.en-standard.eu/bs-en-13284-1-2017-stationary-source-emissions-determination-of-low-range-mass-concentration-of-dust-manual-gravimetric-method/?gad_source=1&gclid=CjwKCAjw34qzBhBmEiwAOUQcF1uQOeH0x68EgcOWp5Xj0EwxUNaXg5iOjzjnKQ-BpJ2OD7HgUipbgBoC (accessed on 11 September 2024).
13. Method 201A—PM10 and PM2.5—Constant Sampling Rate Procedure | US EPA. Available online: https://www.epa.gov/emc/method-201a-pm10-and-pm25-constant-sampling-rate-procedure (accessed on 11 September 2024).
14. Saraswati. Characterization of Primary and Secondary Airborne Particulates. In *Airborne Particulate Matter: Source, Chemistry and Health*; Springer: Singapore, 2022; pp. 103–129. [CrossRef]
15. Rodríguez Rama, J.A.; Presa Madrigal, L.; Costafreda Mustelier, J.L.; García Laso, A.; Maroto Lorenzo, J.; Martín Sánchez, D.A. Monitoring and Ensuring Worker Health in Controlled Environments Using Economical Particle Sensors. *Sensors* **2024**, *24*, 5267. [CrossRef]
16. Li, J.; Biswas, P. Optical Characterization Studies of a Low-Cost Particle Sensor. *Aerosol Air Qual. Res.* **2017**, *17*, 1691–1704. [CrossRef]
17. Concas, F.; Mineraud, J.; Lagerspetz, E.; Varjonen, S.; Liu, X.; Puolamäki, K.; Nurmi, P.; Tarkoma, S. Low-Cost Outdoor Air Quality Monitoring and Sensor Calibration. *ACM Trans. Sens. Networks* **2021**, *17*, 1–44. [CrossRef]
18. Felici-Castell, S.; Segura-Garcia, J.; Perez-Solano, J.J.; Fayos-Jordan, R.; Soriano-Asensi, A.; Alcaraz-Calero, J.M. AI-IoT Low-Cost Pollution-Monitoring Sensor Network to Assist Citizens with Respiratory Problems. *Sensors* **2023**, *23*, 9585. [CrossRef] [PubMed]

19. Bulot, F.M.J.; Russell, H.S.; Rezaei, M.; Johnson, M.S.; Ossont, S.J.; Morris, A.K.R.; Basford, P.J.; Easton, N.H.C.; Mitchell, H.L.; Foster, G.L.; et al. Laboratory Comparison of Low-Cost Particulate Matter Sensors to Measure Transient Events of Pollution—Part B—Particle Number Concentrations. *Sensors* **2023**, *23*, 7657. [CrossRef] [PubMed]
20. Schneider, P.; Vogt, M.; Haugen, R.; Hassani, A.; Castell, N.; Dauge, F.R.; Bartonova, A. Deployment and Evaluation of a Network of Open Low-Cost Air Quality Sensor Systems. *Atmosphere* **2023**, *14*, 540. [CrossRef]
21. Kumar, P.; Morawska, L.; Martani, C.; Biskos, G.; Neophytou, M.; Di Sabatino, S.; Bell, M.; Norford, L.; Britter, R. The Rise of Low-Cost Sensing for Managing Air Pollution in Cities. *Environ. Int.* **2015**, *75*, 199–205. [CrossRef]
22. Castell, N.; Dauge, F.R.; Schneider, P.; Vogt, M.; Lerner, U.; Fishbain, B.; Broday, D.; Bartonova, A. Can Commercial Low-Cost Sensor Platforms Contribute to Air Quality Monitoring and Exposure Estimates? *Environ. Int.* **2017**, *99*, 293–302. [CrossRef]
23. Popoola, O.A.M.; Lad, C.; Vivien, B.; Bright, D.C.; Mohammed, I. Meada John, R.; Saffelld, Roderic, L.; Jones, M.E.J.S. Use of Networks of Low Cost Air Quality Sensors to Quantify Air Quality in Urban Settings. *Atmos. Environ.* **2018**, *194*, 58–70. [CrossRef]
24. Karagulian, F.; Barbiere, M.; Kotsev, A.; Spinelle, L.; Gerboles, M.; Lagler, F.; Redon, N.; Crunaire, S.; Borowiak, A. Review of the Performance of Low-Cost Sensors for Air Quality Monitoring. *Atmosphere* **2019**, *10*, 506. [CrossRef]
25. Giordano, M.R.; Malings, C.; Pandis, S.N.; Presto, A.A.; McNeill, V.F.; Westervelt, D.M.; Beekmann, M.; Subramanian, R. From Low-Cost Sensors to High-Quality Data: A Summary of Challenges and Best Practices for Effectively Calibrating Low-Cost Particulate Matter Mass Sensors. *J. Aerosol Sci.* **2021**, *158*, 105833. [CrossRef]
26. Kang, Y.; Aye, L.; Ngo, T.D.; Zhou, J. Performance Evaluation of Low-Cost Air Quality Sensors: A Review. *Sci. Total Environ.* **2022**, *818*, 151769. [CrossRef]
27. Frederickson, L.B.; Russell, H.S.; Sørensen, M.O.B.; Schmidt, J.A.; Hertel, O.; Johnson, M.S. Hyperlocal Air Pollution in London Part 2: NO2 with a Low-Cost Sensor Network andMobile Monitoring. *ChemRxiv* **2024**. [CrossRef]
28. Jaafar, W.; Xu, J.; Farrar, E.; Jeong, C.H.; Ganji, A.; Evans, G.; Hatzopoulou, M. Challenges and Opportunities of Low-Cost Sensors in Capturing the Impacts of Construction Activities on Neighborhood Air Quality. *Build. Environ.* **2024**, *254*, 111363. [CrossRef]
29. Stojanović, D.B.; Kleut, D.; Davidović, M.; Živković, M.; Ramadani, U.; Jovanović, M.; Lazović, I.; Jovašević-Stojanović, M. Data Evaluation of a Low-Cost Sensor Network for Atmospheric Particulate Matter Monitoring in 15 Municipalities in Serbia. *Sensors* **2024**, *24*, 4052. [CrossRef] [PubMed]
30. Samad, A.; Kieser, J.; Chourdakis, I.; Vogt, U. Developing a Cloud-Based Air Quality Monitoring Platform Using Low-Cost Sensors. *Sensors* **2024**, *24*, 945. [CrossRef] [PubMed]
31. Pritchard, H.; Gabrys, J.; Houston, L. Re-Calibrating DIY: Testing Digital Participation across Dust Sensors, Fry Pans and Environmental Pollution. *New Media Soc.* **2018**, *20*, 4533–4552. [CrossRef]
32. Alfano, B.; Barretta, L.; Del Giudice, A.; De Vito, S.; Di Francia, G.; Esposito, E.; Formisano, F.; Massera, E.; Miglietta, M.L.; Polichetti, T. A Review of Low-Cost Particulate Matter Sensors from the Developers' Perspectives. *Sensors* **2020**, *20*, 1–56. [CrossRef]
33. Vercauteren, J. *Performance Evaluation of Six Low-Cost Particulate Matter Sensors in the Field*; VAQUUMS: Antwerp, Belgium, 2021.
34. Kaur, K.; Kelly, K.E. Laboratory Evaluation of the Alphasense OPC-N3, and the Plantower PMS5003 and PMS6003 Sensors. *J. Aerosol Sci.* **2023**, *171*, 106181. [CrossRef]
35. Alphasense. Available online: https://www.alphasense.com/products/ (accessed on 5 October 2024).
36. Alvarez Cruz, A.; Morales Pérez, M.C.; Alejo Sánchez, D.; Rivero, R.A.G.; Santana, L.H. Evaluación Comparativa de Sensores de Partículas En Santa Clara, Cuba. *Ing. Electrónica Automática Comun.* **2023**, *44*, 24–34.
37. Kosmopoulos, G.; Salamalikis, V.; Pandis, S.N.; Yannopoulos, P.; Bloutsos, A.A.; Kazantzidis, A. Low-Cost Sensors for Measuring Airborne Particulate Matter: Field Evaluation and Calibration at a South-Eastern European Site. *Sci. Total Environ.* **2020**, *748*, 141396. [CrossRef]
38. Araújo, T.; Silva, L.; Moreira, A. Evaluation of Low-Cost Sensors for Weather and Carbon Dioxide Monitoring in Internet of Things Context. *IoT* **2020**, *1*, 286–308. [CrossRef]
39. Liang, L. Calibrating Low-Cost Sensors for Ambient Air Monitoring: Techniques, Trends, and Challenges. *Environ. Res.* **2021**, *197*, 111163. [CrossRef] [PubMed]
40. Mendez, E.; Temby, O.; Wladyka, D.; Sepielak, K.; Raysoni, A.U. Using Low-Cost Sensors to Assess PM2.5 Concentrations at Four South Texan Cities on the U.S.—Mexico Border. *Atmosphere* **2022**, *13*, 1554. [CrossRef]
41. Dubey, R.; Patra, A.K.; Joshi, J.; Blankenberg, D.; Kolluru, S.S.R.; Madhu, B.; Raval, S. Evaluation of Low-Cost Particulate Matter Sensors OPC N2 and PM Nova for Aerosol Monitoring. *Atmos. Pollut. Res.* **2022**, *13*. [CrossRef]
42. Aix, M.L.; Schmitz, S.; Bicout, D.J. Calibration Methodology of Low-Cost Sensors for High-Quality Monitoring of Fine Particulate Matter. *Sci. Total Environ.* **2023**, *889*, 164063. [CrossRef]
43. Christakis, I.; Tsakiridis, O.; Kandris, D.; Stavrakas, I. A Kalman Filter Scheme for the Optimization of Low-Cost Gas Sensor Measurements. *Electronics* **2023**, *13*, 25. [CrossRef]
44. Wang, G.; Yu, C.; Guo, K.; Guo, H.; Wang, Y. Research of Low-Cost Air Quality Monitoring Models with Different Machine Learning Algorithms. *Atmos. Meas. Tech.* **2024**, *17*, 181–196. [CrossRef]

45. Kairuz-Cabrera, D.; Hernandez-Rodriguez, V.; Schalm, O.; Martinez, A.; Laso, P.M.; Alejo-Sánchez, D. Development of a Unified IoT Platform for Assessing Meteorological and Air Quality Data in a Tropical Environment. *Sensors* **2024**, *24*, 2729. [CrossRef]
46. Bulot, F.M.J.; Johnston, S.J.; Basford, P.J.; Easton, N.H.C.; Apetroaie-Cristea, M.; Foster, G.L.; Morris, A.K.R.; Cox, S.J.; Loxham, M. Long-Term Field Comparison of Multiple Low-Cost Particulate Matter Sensors in an Outdoor Urban Environment. *Sci. Rep.* **2019**, *9*, 1–13. [CrossRef]
47. Bulot, F.M.J.; Russell, H.S.; Rezaei, M.; Johnson, M.S.; Ossont, S.J.J.; Morris, A.K.R.; Basford, P.J.; Easton, N.H.C.; Foster, G.L.; Loxham, M.; et al. Laboratory Comparison of Low-Cost Particulate Matter Sensors to Measure Transient Events of Pollution. *Sensors* **2020**, *20*, 2219. [CrossRef]
48. Báthory, C.; Dobó, Z.; Garami, A.; Palotás, Á.; Tóth, P. Low-Cost Monitoring of Atmospheric PM—Development and Testing. *J. Environ. Manag.* **2022**, *304*, 114158. [CrossRef]
49. Kaur, K.; Kelly, K.E. Performance Evaluation of the Alphasense OPC-N3 and Plantower PMS5003 Sensor in Measuring Dust Events in the Salt Lake Valley, Utah. *Atmos. Meas. Tech.* **2023**, *16*, 2455–2470. [CrossRef]
50. Penchala, A.; Patra, A.K.; Mishra, N.; Santra, S. Field Calibration and Performance Evaluation of Low-Cost Sensors for Monitoring Airborne PM in the Occupational Mining Environment. *J. Aerosol. Sci.* **2025**, *184*, 106519. [CrossRef]
51. Bruchkouski, I.; Szkop, A.; Wink, J.; Szymkowska, J.; Pietruczuk, A. Multi-Sensor Instrument for Aerosol In Situ Measurements. *Atmos.* **2025**, *16*, 42. [CrossRef]
52. Reliford, A.; Smith, S.T.; Osei-Ntansah, K.; Stewart, A.; Jackson, D. From Calibration to Flight: Assessing the Alphasense OPC-N3 for Aerial Data Collection. In Proceedings of the AIAA SCITECH 2025 Forum 2025, Orlando, FL, USA, 6–10 January 2025.
53. Hernández-Rodríguez, E.; Schalm, O.; Martínez, A. Development of A Low-Cost Measuring System for the Monitoring of Environmental Parameters that Affect Air Quality for Human Health. *ITEGAM-JETIA* **2020**, *6*, 22–27. [CrossRef]
54. Sun, J.; Besant, R.W. Heat and Mass Transfer during Silica Gel-Moisture Interactions. *Int. J. Heat Mass Transf.* **2005**, *48*, 4953–4962. [CrossRef]
55. Jagatha, J.V.; Klausnitzer, A.; Chacón-Mateos, M.; Laquai, B.; Nieuwkoop, E.; van der Mark, P.; Vogt, U.; Schneider, C. Calibration Method for Particulate Matter Low-Cost Sensors Used in Ambient Air Quality Monitoring and Research. *Sensors* **2021**, *21*, 3960. [CrossRef]
56. Morera-Gómez, Y.; Alonso-Hernández, C.M.; Santamaría, J.M.; Elustondo, D.; Lasheras, E.; Widory, D. Levels, Spatial Distribution, Risk Assessment, and Sources of Environmental Contamination Vectored by Road Dust in Cienfuegos (Cuba) Revealed by Chemical and C and N Stable Isotope Compositions. *Environ. Sci. Pollut. Res.* **2020**, *27*, 2184–2196. [CrossRef]
57. Morera-Gómez, Y.; Alonso-Hernández, C.M.; Armas-Camejo, A.; Viera-Ribot, O.; Morales, M.C.; Alejo, D.; Elustondo, D.; Lasheras, E.; Santamaría, J.M. Pollution Monitoring in Two Urban Areas of Cuba by Using *Tillandsia recurvata* (L.) L. and Top Soil Samples: Spatial Distribution and Sources. *Ecol. Indic.* **2021**, *126*, 107667. [CrossRef]
58. Morera-Gómez, Y.; Santamaría, J.M.; Elustondo, D.; Lasheras, E.; Alonso-Hernández, C.M. Determination and Source Apportionment of Major and Trace Elements in Atmospheric Bulk Deposition in a Caribbean Rural Area. *Atmos. Environ.* **2019**, *202*, 93–104. [CrossRef]
59. González, R.R.A.; Schalm, O.; Alvarez Cruz, A.; Hernández Rodríguez, E.; Morales Pérez, M.C.; Alejo Sánchez, D.; Martinez Laguardia, A.; Jacobs, W.; Hernández Santana, L. Relevance and Reliability of Outdoor SO2 Monitoring in Low-Income Countries Using Low-Cost Sensors. *Atmosphere* **2023**, *14*, 912. [CrossRef]
60. Hernández-Rodríguez, E.; González-Rivero, R.A.; Schalm, O.; Martínez, A.; Hernández, L.; Alejo-Sánchez, D.; Janssens, T.; Jacobs, W. Reliability Testing of a Low-Cost, Multi-Purpose Arduino-Based Data Logger Deployed in Several Applications Such as Outdoor Air Quality, Human Activity, Motion, and Exhaust Gas Monitoring. *Sensors* **2023**, *23*, 7412. [CrossRef] [PubMed]
61. NC:111. Calidad Del Aire. In *Reglas Para La Vigilancia de La Calidad Del Aire En Asentamientos Humanos*; Oficina Nacional de Normalización: La Habana, Cuba, 2004.
62. Ahrens, L.H. The Lognormal Distribution of the Elements (A Fundamental Law of Geochemistry and Its Subsidiary). *Geochim. Cosmochim. Acta* **1954**, *5*, 49–73. [CrossRef]
63. Latham, A.G.; Harding, K.L.; Lapointe, P.; Morris, W.A.; Balch, S.J. On the Lognormal Distribution of Oxides in Igneous Rocks, Using Magnetic Susceptibility as a Proxy for Oxide Mineral Concentration. *Geophys. J. Int.* **1989**, *96*, 179–184. [CrossRef]
64. Andersson, A. Mechanisms for Log Normal Concentration Distributions in the Environment. *Sci. Rep.* **2021**, *11*, 1–7. [CrossRef]
65. Zhu, F.; Qin, B.; Feng, W.; Wang, H.; Huang, S.; Lv, Y.; Chen, Y. Reducing Poisson Noise and Baseline Drift in X-Ray Spectral Images with Bootstrap Poisson Regression and Robust Nonparametric Regression. *Phys. Med. Biol.* **2013**, *58*. [CrossRef]
66. Kang, J.; Choi, K. Calibration Methods for Low-Cost Particulate Matter Sensors Considering Seasonal Variability. *Sensors* **2024**, *24*, 3023. [CrossRef]
67. Schalm, O.; Carro, G.; Lazarov, B.; Jacobs, W.; Stranger, M. Reliability of Lower-Cost Sensors in the Analysis of Indoor Air Quality on Board Ships. *Atmosphere* **2022**, *13*, 1579. [CrossRef]
68. Nurowska, K.; Mohammadi, M.; Malinowski, S.; Markowicz, K. Applicability of the Low-Cost OPC-N3 Optical Particle Counter for Microphysical Measurements of Fog. *Atmos. Meas. Tech.* **2023**, *16*, 2415–2430. [CrossRef]

69. Hapidin, D.A.; Saputra, C.; Maulana, D.S.; Munir, M.M.; Khairurrijal, K. Aerosol Chamber Characterization for Commercial Particulate Matter (PM) Sensor Evaluation. *Aerosol Air Qual. Res.* **2019**, *19*, 181–194. [CrossRef]
70. Stavroulas, I.; Grivas, G.; Michalopoulos, P.; Liakakou, E.; Bougiatioti, A.; Kalkavouras, P.; Fameli, K.M.; Hatzianastassiou, N.; Mihalopoulos, N.; Gerasopoulos, E. Field Evaluation of Low-Cost PM Sensors (Purple Air PA-II) Under Variable Urban Air Quality Conditions, in Greece. *Atmosphere* **2020**, *11*, 926. [CrossRef]
71. Chacón-Mateos, M.; Laquai, B.; Vogt, U.; Stubenrauch, C. Evaluation of a Low-Cost Dryer for a Low-Cost Optical Particle Counter. *Atmos. Meas. Tech.* **2022**, *15*, 7395–7410. [CrossRef]
72. Nurowska, K.; Markowicz, K.M. Determination of Hygroscopic Aerosol Growth Based on the OPC-N3 Counter. *Atmosphere* **2024**, *15*, 61. [CrossRef]
73. Ørby, P.V.; Andersen, J.L.; Ottosen, T.B.; Thrane, U.; Gosewinkel, U. Detection of a Biological Aerosol Using Optical Particle Counters. *Atmos. Environ.* **2024**, *338*, 120819. [CrossRef]
74. Lopez de Ipiña, J.M.; Lopez, A.; Gazulla, A.; Aznar, G.; Belosi, F.; Koivisto, J.; Seddon, R.; Durałek, P.; Vavouliotis, A.; Koutsoukis, G.; et al. Field Testing of Low-Cost Particulate Matter Sensors for Digital Twin Applications in Nanomanufacturing Processes. *J. Phys. Conf. Ser.* **2024**, *2695*, 012002. [CrossRef]